Short Communication

Lysophosphatidylcholine activates caspase-1 in microglia via a novel pathway involving two inflammasomes

Holger Scholz, Claudia Eder [a*]

Charité – Universitätsmedizin Berlin, Institute of Physiology, 10117 Berlin, Germany

[a] Present address: St. George's, University of London; London SW17 0RE; UK

* Corresponding author at: St. George's, University of London; Cranmer Terrace; London SW17 0RE; UK. E-mail address: ceder@sgul.ac.uk (C. Eder)

Abbreviations: ASC, apoptosis-associated speck-like protein containing a caspase activation and recruitment domain; DAMPs, damage-associated molecular patterns; IL, interleukin; LPC, lysophosphatidylcholine; LPS, lipopolysaccharide; NLRC4, nucleotide-binding domain and leucine-rich repeat caspase recruitment domain 4; NLRP3, nucleotide-binding domain and leucine-rich pyrin domain 3; PAMPs, pathogen-associated molecular patterns

ABSTRACT

Inflammasomes regulate microglial caspase-1 activation and subsequent neuroinflammatory processes in brain pathology. In the present study, we have identified inflammasomes causing caspase-1 activation following stimulation of microglia with lysophosphatidylcholine (LPC), a proinflammatory lipid generated under pathological conditions in the brain. LPC-induced caspase-1 activation in microglia was found to depend on LPS prestimulation, inflammasome NLRP3 and adaptor molecule ASC. Furthermore, knockdown of inflammasome NLRC4 inhibited LPC-stimulated caspase-1 activity in microglia, suggesting the requirement of two inflammasomes for optimal caspase-1 activity.

Key words: microglia, caspase-1, inflammasome, lysophospholipids

1. Introduction

Caspase-1 has been considered as a potential therapeutic target in a variety of neurological diseases (Vezzani et al., 2010; Walsh et al., 2014; Song et al., 2017). It converts biologically inactive precursors of the proinflammatory cytokines interleukin (IL)-1β, IL-18 and IL-33 into their mature, biologically active forms, which play a pivotal role in promoting neuroinflammatory processes (Eder, 2009; Garlanda et al., 2013). Mechanisms underlying caspase-1 activation in microglia are not completely understood. Multiple pathways can lead to caspase-1 activation in microglia, while intracellular protein complexes called inflammasomes are major components of the activation cascade of caspase-1 (Walsh et al., 2014; Song et al., 2017).

Lysophosphatidylcholine (LPC) is a proinflammatory lipid, which is released from apoptotic cells or produced under inflammatory or ischemic conditions in the brain as a result of enhanced phospholipase A_2 activity (Farooqui and Harrocks, 2006; Drzazga et al., 2014).

LPC can cause microglial recruitment during brain development (Xu et al., 2016) and microglial activation in brain pathology (Inose et al., 2015). We have previously demonstrated that LPC induces caspase-1 activation in microglia (Stock et al., 2006), which depends on Na^+ influx, reactive oxygen species production and intact lipid rafts (Schilling and Eder, 2010, 2011). Here, we have extended our studies and identified inflammasomes regulating LPC-stimulated caspase-1 activity in microglia.

2. Materials and methods

2.1. Materials

The following drugs were used in this study: synthetic L-α-lysophosphatidylcholine (LPC), palmitoyl (16:0); lipopolysaccharide (LPS) from E. coli 055:B5 (both from Sigma-Aldrich, Germany). Stock solutions of 30 mM LPC and 1 mg/ml LPS were prepared in H_2O.

2.2. Cells

All experiments were performed on the microglial cell line BV-2. Cells were cultured permanently in DMEM supplemented with 10% FCS and 2 mM L-glutamine as described previously (Stock et al., 2006). Cells were split twice a week, and were plated on glass coverslips at a density of $1x10^5$/ml for subsequent experiments. During experiments, cells were maintained in an extracellular solution containing (in mM): NaCl, 130; KCl, 5; $CaCl_2$, 2; $MgCl_2$, 1; HEPES, 10; D-glucose, 10 (pH 7.4) as described previously (Stock et al., 2006; Schilling et al., 2010, 2011).

2.3. siRNA-induced knockdown of NLRC4, NLRP3 and ASC

One day before transfection with siRNA, BV-2 microglial cells were seeded in 35 mm petri dishes at a density of $3x10^5$/ml and maintained in DMEM supplemented with 10% FCS

and 2 mM L-glutamine. The siRNAs for targeting the murine mRNAs of *ASC* (NCBI accession number NM_023258), *NLRC4* (NCBI accession number NM_001033367) and *NLRP3* (NCBI accession number AY355340) were synthesized by Xeragon/Qiagen (Köln, Germany). Sequences of siRNAs are provided in table 1. A non-targeting (scrambled) siRNA (200 pmoles per dish) was used as a negative control. To achieve maximum efficiencies of gene silencing, cells were transfected with a mixture of 4 different siRNAs, each at 50 pmoles per dish. For this purpose, siRNAs were diluted at a 1:20 volume ratio in 0.2 ml serum-free DMEM, and the DharmaFECT® transfection reagent (Perbio Science, Bonn, Germany) was diluted 1:100 in 0.2 ml serum-free DMEM. Diluted siRNAs and the transfection reagent were combined and kept at room temperature for 20 min to allow complex formation. In the meantime, the culture medium was removed from cells and replaced with 1.6 ml fresh DMEM/10% FCS. The siRNA transfection mixtures (0.4 ml) were carefully added to the cells, which were subsequently maintained in a cell culture incubator for 24 hours.

Detection of *NLRC4* mRNA, *NLRP3* mRNA and *ASC* mRNA, and their downregulation by the corresponding siRNAs were verified by reverse transcription real-time PCR. Total RNA was isolated from cultured cells by the use of TRIzol® reagent (Invitrogen, Karlsruhe, Germany) according to the manufacturer's protocol. First-strand cDNA synthesis was performed with 2 µg of total RNA using oligo(dT) primers and Superscript II reverse transcriptase (Invitrogen). Five percent of the volumes of the reaction products were used for quantitative real-time PCR amplification with SYBR® Green PCR Master Mix (Applied Biosystems, Foster City, CA). PCRs were carried out on a GeneAmp5700 thermocycler (PerkinElmer Life Sciences) under the following conditions (45 cycles): DNA denaturation (15 s) at 94 °C, primer annealing (15 s) and extension of double-stranded DNA at 60 °C (60 s), detection of SYBR® Green fluorescence at 77 °C (30 s). PCR primers used for the

amplification reactions are listed in table 2. Threshold cycle (Ct) values for the genes of interest were subtracted from Ct values for *GAPDH* to obtain δCt values. Differences in transcript levels between cells transfected with gene-specific siRNAs and scrambled siRNA, respectively, were calculated as δCt(gene of interest) - δCt(scrambled). Fold increases in mRNA levels were obtained according to $2^{\delta\delta Ct}$ as described in detail previously (Martens et al., 2007). Pretreatment of BV-2 cells with *NLRC4* siRNA, *NLRP3* siRNA or *ASC* siRNA caused specific reduction in the corresponding mRNA levels by 82.4±15.2%, 56.8±17.6% and 78.2±13.4%, respectively (n=3 experiments in each case), compared to cells that had been incubated with scrambled siRNA.

2.4. Detection of caspase-1 activity

Activity of caspase-1 was revealed by FAM-YVAD-FMK (1:150; Immunochemistry Technology, Bloomington, USA) using a fluorescence imaging system as described previously (Stock et al., 2006; Schilling and Eder, 2010, 2011). Images of four different visual fields for three independent experiments per condition were collected and analyzed. Fluorescence intensities of all cells were corrected for background fluorescence.

2.5. Statistics

All data are presented as mean values ± standard error of the mean (SEM) and cell numbers are indicated. The statistical significance of differences between experimental groups was evaluated by one-way ANOVA using the SPSS program. Tukey's test was used for post hoc comparison after confirming homogeneity of variances with Levene's test. Data were considered to be statistically significant with $p<0.05$.

3. Results

3.1. LPC-induced caspase-1 activity requires LPS pretreatment

As demonstrated in Fig. 1A-B, LPC caused substantial increases in caspase-1 activity in microglial cells pretreated with 1 μg/ml LPS for 6 h. In comparison with unstimulated control cells, mean fluorescence intensity of microglial cells stimulated with 30 μM LPC for 1 h was significantly increased to 381.0±7.5% (n=482 cells of 3 independent experiments; $p<0.001$). In contrast, without LPS pretreatment, mean fluorescence intensities did not differ markedly between cells maintained either in the presence or absence of 30 μM LPC for 1 h (Fig. 1C-D). Due to the requirement of LPS pretreatment for LPC-induced caspase-1 activity, microglial cells were exposed to 1 μg/ml LPS for 6 h prior to LPC stimulation in all further experiments.

3.2. LPC-induced caspase-1 activity requires NLRC4, NLRP3 and ASC

To further identify mechanisms underlying LPC-stimulated caspase-1 activity, we tested whether siRNA-induced knockdown of the inflammasome NLRC4, the inflammasome NLRP3 and/or the adaptor protein ASC affect caspase-1 activation in LPC-stimulated microglia. As shown in Fig. 2, control experiments revealed that transfection of cells with non-targeting (scrambled) siRNA did not affect LPC-induced caspase-1 activation. Similar to data obtained in microglial cells that had not been exposed to scrambled siRNA (Fig. 1), FAM-YVAD-FMK fluorescence intensity of microglia pretreated with scrambled siRNA for 24 h increased 4-fold (to 384.3±10.0%; n=555 cells of 3 independent experiments; $p<0.001$) in response to stimulation of cells with 30 μM LPC (Fig. 2).

Following siRNA-induced knockdown of inflammasomes NLRC4 or NLRP3, caspase-1 activity was significantly inhibited (Fig. 2), indicating the involvement of both inflammasomes in microglial LPC-stimulated caspase-1 activation. In comparison with LPC-

stimulated microglia pretreated with scrambled siRNA, mean FAM-YVAD-FMK fluorescence intensities were reduced by 69.8±1.0% (n=526 cells of 3 independent experiments; $p<0.001$) or by 35.3±1.6% (n=541 cells of 3 independent experiments; $p<0.001$) in LPC-stimulated microglia pretreated with *NLRC4* siRNA or with *NLRP3* siRNA, respectively. We additionally tested efficiency and specificity of siRNAs in cells stimulated with ATP. As expected and published by others previously (e.g., Freeman et al., 2017; Song et al., 2017), stimulation with 2 mM ATP increased caspase-1 activity in microglia 6-fold (to 625.8±19.3%, n=562 cells of 3 independent experiments; $p<0.001$), while *NLRP3* siRNA, but not *NLRC4* siRNA, reduced ATP-induced caspase-1 activity by 80.2±3% (n=546 cells of 3 independent experiments; $p<0.001$).

Furthermore, siRNA knockdown experiments revealed that in addition to the inflammasomes NLRC4 and NLRP3, the adaptor protein ASC mainly contributes to caspase-1 activity in LPC-stimulated microglia. In LPC-stimulated microglial cells pretreated with *ASC* siRNA, mean FAM-YVAD-FMK fluorescence intensity was reduced by 68.6±1.0% (n=542 cells of 3 independent experiments; $p<0.001$) compared to LPC-stimulated microglial cells pretreated with scrambled siRNA for 24 h (Fig. 2). Independent of pretreatment conditions, caspase-1 activity of LPC-stimulated microglia was significantly larger ($p<0.001$ in all cases) than that of unstimulated microglia pretreated with scrambled siRNA (Fig. 2).

4. Discussion

In the present study, we have unraveled a novel mechanism of caspase-1 activation in microglia, which was triggered by LPC, a recognized damage-associated molecular pattern (DAMP) generated in a variety of neurological diseases. It has been shown previously that DAMPs, such as ATP or amyloid-β, cause caspase-1 activity in LPS-pretreated microglia exclusively via the inflammasome NLRP3 (Walsh et al., 2017). The inflammasome NLRC4

has only recently been identified in microglia (Jamilloux et al., 2013; Lammerding et al., 2016; Freeman et al., 2017), and could be activated in cultured microglial cells following transfection with the pathogen-associated molecular pattern (PAMP) *Legionella pneumonia* (Jamilloux et al., 2013). Similar to stimulation with other DAMPs, in LPC-stimulated microglial cells, LPS pretreatment was required to trigger caspase-1 activity. However, in contrast to microglial caspase-1 activation induced by other DAMPs, two inflammasomes, namely NLRC4 and NLRP3, were found to regulate LPC-induced microglial caspase-1 activity. Similar to our findings on microglia, a recent study performed on LPC-stimulated astrocytes reported reduced IL-1β secretion from cells of *NLRC4* or *NLRP3* knockout mice (Freeman et al., 2017), suggesting the involvement of both inflammasomes in caspase-1 activation of astrocytes. In the past, numerous studies have suggested that the inflammasome NLRC4 is predominantly activated by PAMPs (Zhao and Shao, 2015; Vance, 2015).

What might be the reason for the activation of caspase-1 by LPC in microglia via a distinct pathway not used by other DAMPs? Intriguingly, LPC can exert its effects via multiple mechanisms, while it can act both extracellularly and intracellularly. Extracellular effects of LPC are mediated following binding to membrane receptors (Inose et al., 2015; Xu et al., 2016) and/or by changing the membrane curvature and subsequent activation of mechanosensitive non-selective cation channels (Perozo et al., 2002; Vásquez et al., 2008). Furthermore, unlike other DAMPs, LPC is capable of crossing the cell membrane (van der Luit et al., 2003). Thus, it is possible that LPC, like PAMPs, can directly interact intracellularly with the NLRC4 inflammasome after its internalization. In addition, LPC-induced activation of non-selective cation channels, which mediate Na^+ and Ca^{2+} influx as well as K^+ efflux, could trigger activation of the inflammasome NLRP3, as has been shown for other DAMPs (Walsh et al., 2014; Song et al., 2017). Thus, LPC stimulation may activate

two distinct pathways in parallel, causing simultaneous, but independent, activation of the inflammasomes NLRC4 and NLRP3.

On the other hand, it is also possible that LPC triggers a process similar to that recently described for macrophages infected with *Salmonella typhimurium*, but not other PAMPs. In *Salmonella*-infected cells, both NLRC4 and NLRP3 inflammasomes form a single complex surrounded by the adaptor protein ASC (Broz et al., 2010; Man et al., 2014; Qu et al., 2016). Further work is needed to elucidate the exact mechanism by which LPC activates the two inflammasomes and subsequently caspase-1 in microglia.

Author contribution

CE designed the study. HS performed experiments and analyzed data. CE wrote the manuscript. Both authors approved the final version of the manuscript.

Competing interests

The authors declare that they have no competing interests.

Acknowledgements

We would like to thank Itohan Akhionbare for technical assistance and Dr. Tom Schilling for help with data acquisition and analyses.

Funding

This work was supported by the German Research Foundation DFG (grant SFB 507/C7 to CE).

References

Broz, P., Newton, K., Lamkanfi, M., Mariathasan, S., Dixit, V.M., Monack, D.M., 2010. Redundant roles for inflammasome receptors NLRP3 and NLRC4 in host defense against Salmonella. J. Exp. Med. 207, 1745-1755.

Drzazga, A., Sowińska, A., Koziołkiewicz, M., 2014. Lysophosphatidylcholine and lysophosphatidylinosiol - novel promissing signaling molecules and their possible therapeutic activity. Acta Pol. Pharm. 71, 887-899.

Eder C., 2009. Mechanisms of interleukin-1β release. Immunobiology 214, 543-553.

Farooqui, A.A., Horrocks, L.A., 2006. Phospholipase A_2-generated lipid mediators in the brain: the good, the bad, and the ugly. Neuroscientist 12, 245-260.

Freeman, L., Guo, H., David, C.N., Brickey, W.J., Jha, S., Ting, J.P., 2017. NLR members NLRC4 and NLRP3 mediate sterile inflammasome activation in microglia and astrocytes. J. Exp. Med. 214, 1351-1370.

Garlanda, C., Dinarello, C.A., Mantovani, A., 2013. The interleukin-1 family: back to the future. Immunity 39, 1003-1018.

Inose, Y., Kato, Y., Kitagawa, K., Uchiyama, S., Shibata, N., 2015. Activated microglia in ischemic stroke penumbra upregulate MCP-1 and CCR2 expression in response to lysophosphatidylcholine derived from adjacent neurons and astrocytes. Neuropathology 35, 209-223.

Jamilloux, Y., Pierini, R., Querenet, M., Juruj, C., Fauchais, A.L., Jauberteau, M.O., Jarraud, S., Lina, G., Etienne, J., Roy, C.R., Henry, T., Davoust, N., Ader, F., 2013.

Inflammasome activation restricts Legionella pneumophila replication in primary microglial cells through flagellin detection. Glia 61, 539-549.

Lammerding, L., Slowik, A., Johann, S., Beyer, C., Zendedel, A., 2016. Poststroke inflammasome expression and regulation in the peri-infarct area by gonadal steroids after transient focal ischemia in the rat brain. Neuroendocrinology 103, 460-475.

Man, S.M., Hopkins, L.J., Nugent, E., Cox, S., Glück, I.M., Tourlomousis, P., Wright, J.A., Cicuta, P., Monie, T.P., Bryant, C.E., 2014. Inflammasome activation causes dual recruitment of NLRC4 and NLRP3 to the same macromolecular complex. Proc. Natl. Acad. Sci. 111, 7403-7408.

Martens, L.K., Kirschner, K.M., Warnecke, C., Scholz, H., 2007. Hypoxia-inducible factor-1 (HIF-1) is a transcriptional activator of the TrkB neurotrophin receptor gene. J. Biol. Chem. 282, 14379-14388.

Perozo, E., Kloda, A., Cortes, D.M., Martinac, B., 2002. Physical principles underlying the transduction of bilayer deformation forces during mechanosensitive channel gating. Nat. Struct. Biol. 9, 696-703.

Qu, Y., Misaghi, S., Newton, K., Maltzman, A., Izrael-Tomasevic, A., Arnott, D., Dixit, V.M., 2016. NLRP3 recruitment by NLRC4 during Salmonella infection. J. Exp. Med. 213, 877-885.

Schilling, T., Eder, C., 2010. Importance of lipid rafts for lysophosphatidylcholine-induced caspase-1 activation and reactive oxygen species generation. Cell. Immunol. 265, 87-90.

Schilling, T., Eder, C., 2011. Sodium dependence of lysophosphatidylcholine-induced caspase-1 activity and reactive oxygen species generation. Immunobiology 216, 118-125.

Song, L., Pei, L., Yao, S., Wu, Y., Shang, Y., 2017. NLRP3 Inflammasome in Neurological Diseases, from Functions to Therapies. Front. Cell. Neurosci. 11, 63.

Stock, C., Schilling, T., Schwab, A., Eder, C., 2006. Lysophosphatidylcholine stimulates IL-1β release from microglia via a $P2X_7$ receptor-independent mechanism. J. Immunol. 177, 8560-8568.

Vance, R.E., 2015. The NAIP/NLRC4 inflammasomes. Curr. Opin. Immunol. 32, 84-89.

van der Luit, A.H., Budde, M., Verheij, M., van Blitterswijk, W.J., 2003. Different modes of internalization of apoptotic alkyl-lysophospholipid and cell-rescuing lysophosphatidylcholine. Biochem. J. 374, 747-753.

Vásquez, V., Sotomayor, M., Cordero-Morales, J., Schulten, K., Perozo, E., 2008. A structural mechanism for MscS gating in lipid bilayers. Science 321, 1210-1214.

Vezzani, A., Balosso, S., Maroso, M., Zardoni, D., Noé, F., Ravizza, T., 2010. ICE/caspase 1 inhibitors and IL-1β receptor antagonists as potential therapeutics in epilepsy. Curr. Opin. Investig. Drugs 11, 43-50.

Walsh, J.G., Muruve, D.A., Power, C., 2014. Inflammasomes in the CNS. Nat. Rev. Neurosci. 15, 84-97.

Xu, J., Wang, T., Wu, Y., Jin, W., Wen, Z., 2016. Microglia colonization of developing zebrafish midbrain is promoted by apoptotic neuron and lysophosphatidylcholine. Dev. Cell 38, 214-222.

Zhao, Y., Shao, F., 2015. The NAIP-NLRC4 inflammasome in innate immune detection of bacterial flagellin and type III secretion apparatus. Immunol. Rev. 265, 85-102.

Figure legends

Fig. 1. LPS dependence of LPC-induced caspase-1 activity in microglia. (A) Microglial cells were pretreated with 1 μg/ml LPS for 6 h in DMEM/FCS culture medium, and were subsequently kept untreated or treated with 30 μM LPC for 1 h. Fluorescence intensities (mean values±SEM) of LPC-stimulated microglial cells (n=482) were normalized to the mean fluorescence intensity of untreated control cells (n=621). (B) Brightfield microscopy (upper row) and FAM-YVAD-FMK fluorescence (lower row) images of microglial cells either kept untreated (control) or stimulated with 30 μM LPC (LPC) for 1 h following prestimulation with 1 μg/ml LPS for 6 h. (C) Microglial cells were kept untreated or treated with 30 μM LPC for 1 h without LPS pretreatment. FAM-YVAD-FMK fluorescence intensities (mean values±SEM) of LPC-stimulated microglial cells (n=410) were normalized to the mean fluorescence intensity of untreated control cells (n=418). (D) Brightfield microscopy (upper row) and FAM-YVAD-FMK fluorescence (lower row) images of microglial cells either kept untreated (control) or stimulated with 30 μM LPC (LPC) in the absence of LPS. (B, D) Scale bar, 50 μm.

Fig. 2. Involvement of NLRC4, NLRP3 and ASC in caspase-1 activity in LPC-stimulated microglia. In microglial cells, expression of *NLRC4*, *NLRP3* or *ASC* was silenced by siRNA for 24 h prior to stimulation with 30 μM LPC for 1 h. Fluorescence intensities (mean values±SEM) of LPC-stimulated FAM-YVAD-FMK-loaded microglial cells transfected with non-targeting (scrambled) siRNA (scr; n=942 untreated cells, n=555 LPC-stimulated cells) or *NLRC4* siRNA (NLRC4; n=526), *NLRP3* siRNA (NLRP3; n=541) or *ASC* siRNA (ASC; n=542) were normalized to the mean fluorescence intensity determined for cells transfected

with scrambled siRNA and maintained unstimulated for 1 h. Prior to LPC stimulation, all cells were pretreated with 1μg/ml LPS for 6 hours.

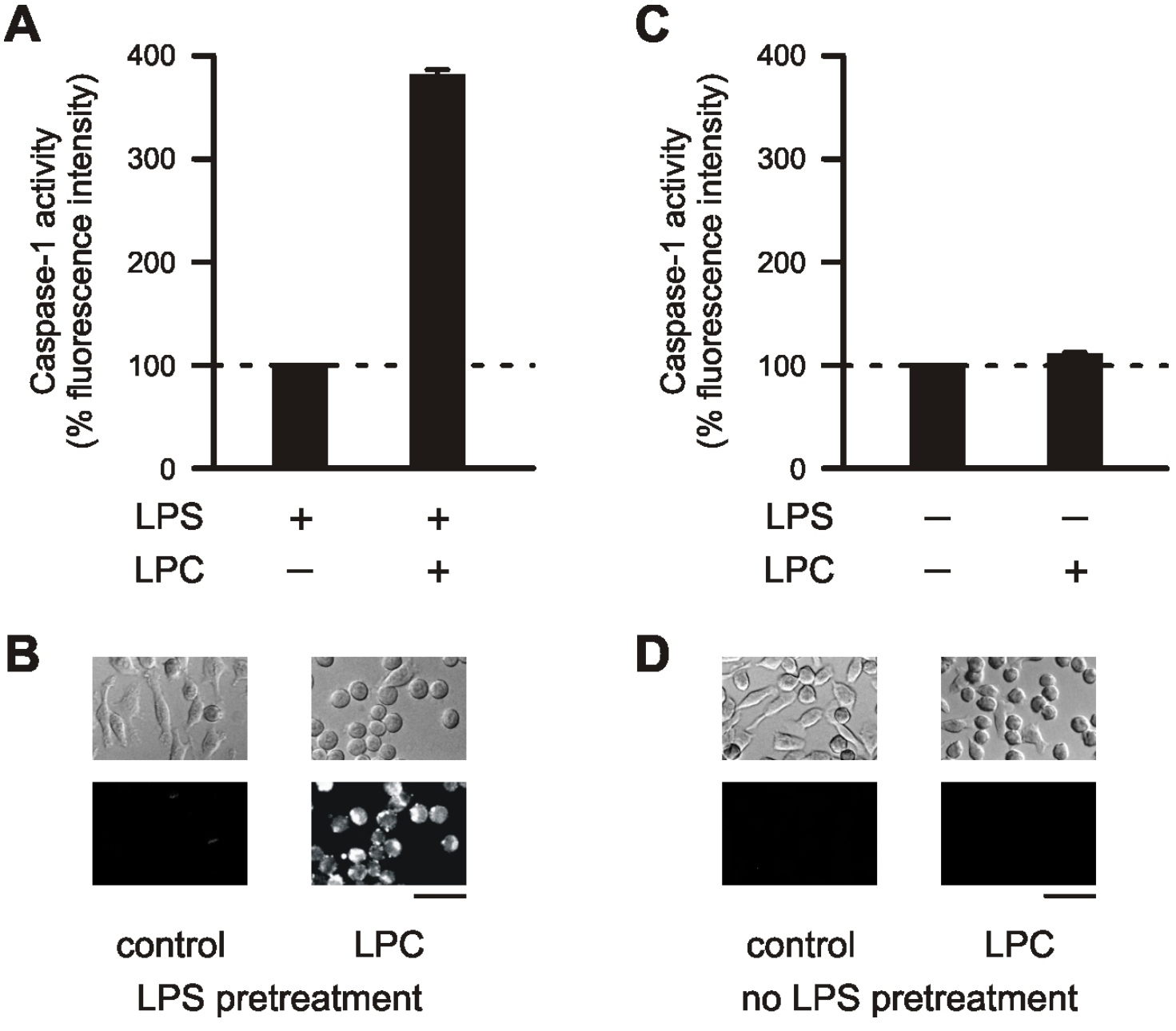
A
Caspase-1 activity
(% fluorescence intensity)
400
300
200
100
0
LPS + +
LPC – +
C
Caspase-1 activity
(% fluorescence intensity)
400
300
200
100
0
LPS – –
LPC – +
B
control
LPC
LPS pretreatment
D
control
LPC
no LPS pretreatment

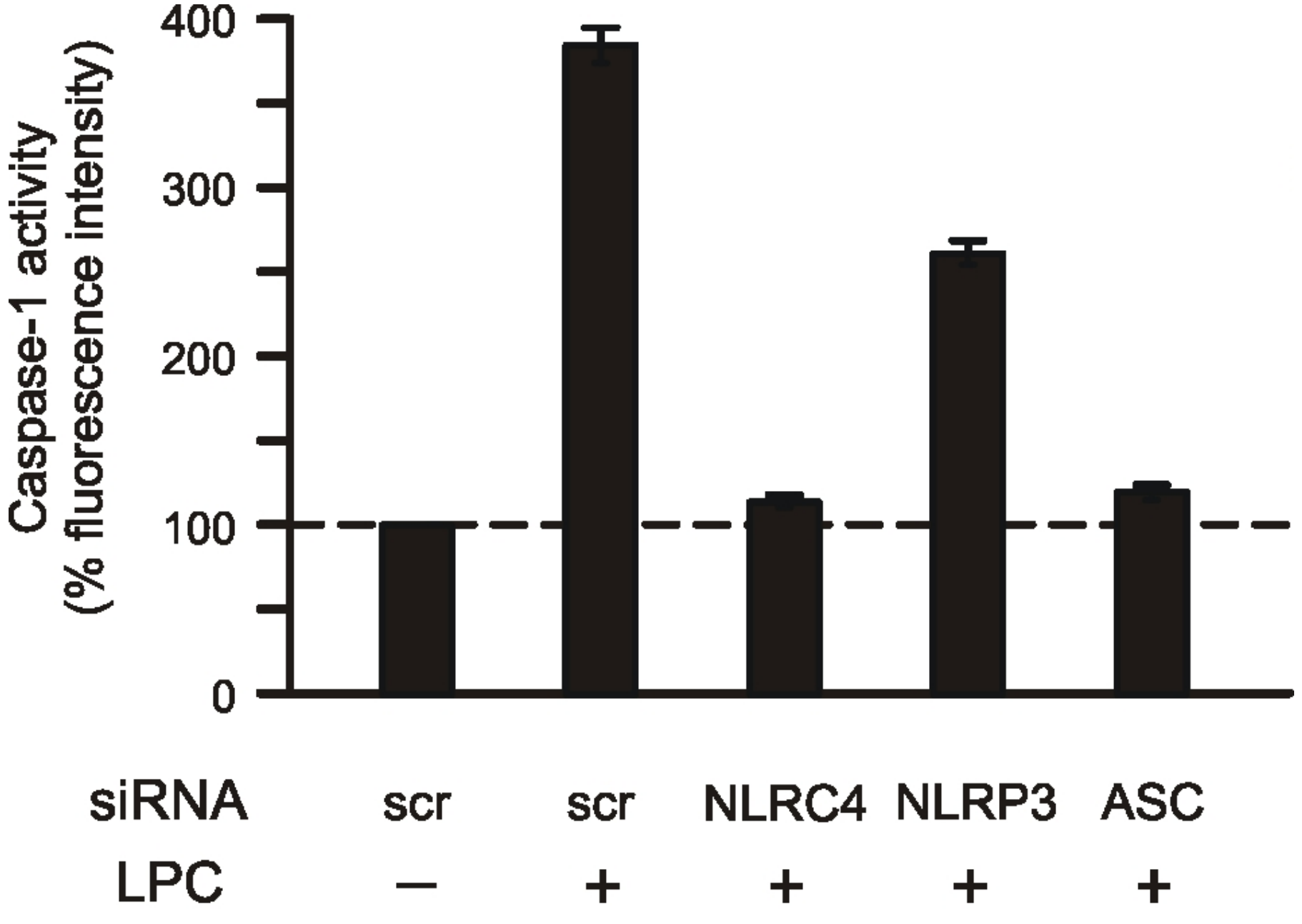
Caspase-1 activity
(% fluorescence intensity)
400
300
200
100
0
siRNA
scr
scr
NLRC4
NLRP3
ASC
LPC
—
+
+
+
+

Table 1. Sequences of the siRNAs used for gene silencing.

Target gene (NCBI accession no.)	siRNA sequences (sense)
ASC/Pycard (NM_023258)	5’-GCUGCAAACGACUAAAGAAdTdT-3’
	5’-GCUACUAUCUGGAGUCGUAdTdT-3’
	5’-CAAUGACUGUGCUUAGAGAdTdT-3’
	5’-CCAGGCCUUGAAGGAAAUAdTdT-3’
NLRC4 (NM_001033367)	5’-GGGUGAAGAUAUCGACAUAdTdT-3’
	5’-GGAUGGGAAUGAAGCUCUAdTdT-3’
	5’-GCUUCUCAACAAUCAAGAAdTdT-3’
	5’-CGUAUAAAUUCUUUCAUAAdTdT-3’
NLRP3 (AY355340)	5’-CCUCUUAUUUGGAGAAGAAdTdT-3’
	5’-GGAUGGCUUUGAUGAGCUAdTdT-3’
	5’-GGAGUAUUUCUUUAAGUAUdTdT-3’
	5’-CCACAAUUCAGACCCACAAdTdT-3’
non-targeting siRNA	5’-UUCUCCGAACGUGUCACGUdTdT-3’

Table 2. Primer sequences used for reverse transcription (RT) PCR of the indicated genes. F - forward primer, R - reverse primer.

mRNA	NCBI accession no.	Oligonucleotide sequence
GAPDH-F	BC083149	5'-ACGACCCCTTCATTGACCTCA-3'
GAPDH-R		5'-TTTGGCTCCACCCTTCAAGTG-3'
ASC (Pycard)-F	NM_023258	5'-CTATCTGGAGTCGTATGGCTTG-3'
ASC (Pycard)-R		5'-CAGGTCCATCACCAAGTAGGG-3'
NLRC4-F	NM_001033367	5'-CAGGTGGTCTGATTGACAGC-3'
NLRC4-R		5'-AAGCCTGCCGATCAGTTCCT-3'
NLRP3-F	AY355340	5'-GCCTGTTCTTCCAGACTGGTG-3'
NLRP3-R		5'-TCTGGAGGTTGCAGAGCAGGT-3'